



Effect of capacitive deionization on disinfection by-product precursors



Danyang Liu^a, Xiaomao Wang^b, Yuefeng F. Xie^{b,c}, Hao L. Tang^{a,d,*}

^a Department of Water Engineering and Science, College of Civil Engineering, Hunan University, Changsha, Hunan 410082, China

^b State Key Joint Laboratory of Environmental Simulation and Pollution Control, School of Environment, Tsinghua University, Beijing 100084, China

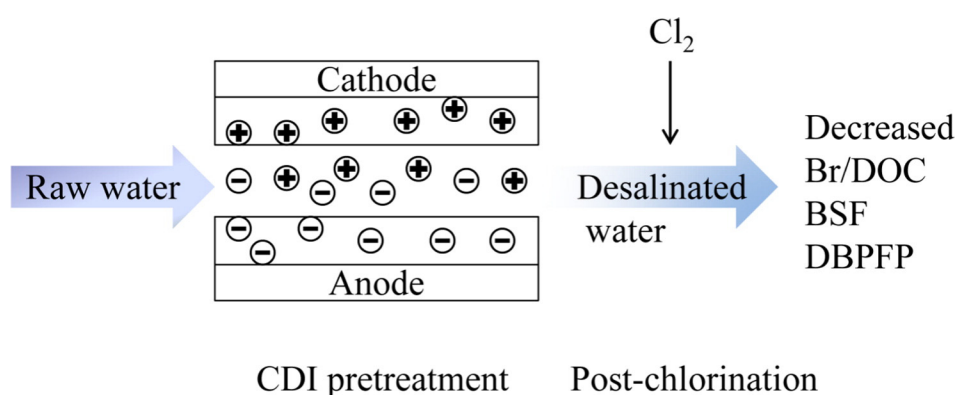
^c Environmental Engineering Programs, Pennsylvania State University, Middletown, PA 17057, USA

^d Department of Chemistry, Indiana University of Pennsylvania, Indiana, PA 15705, USA

HIGHLIGHTS

- Capacitive deionization (CDI) preferentially removed bromide over humic acid.
- DBP formation potential and bromine substitution factors were reduced.
- Mechanisms for DBP precursor removal by CDI treatment were discussed.

GRAPHICAL ABSTRACT



ARTICLE INFO

Article history:

Received 2 May 2016

Received in revised form 30 May 2016

Accepted 31 May 2016

Available online xxxx

Editor: D. Barcelo

Keywords:

Capacitive deionization (CDI)
Disinfection by-product precursor (DBP precursor)
Humic acid
Bromide
Bromine substitution factor (BSF)

ABSTRACT

Formation of brominated disinfection by-products (DBPs) from bromide and natural organic matter upon chlorination imposes health risks to drinking water users. In this study, capacitive deionization (CDI) was evaluated as a potential process for DBP precursor removal. Synthetic humic acid and bromide containing saline water was used as model water prior to CDI treatment. Batch experiments were conducted at cell voltages of 0.6-, 0.9-, and 1.2 V to study the influence of CDI on the ratio of bromide and dissolved organic carbon, bromine substitution factor, and DBP formation potential (FP). Results showed beneficial aspects of CDI on reducing the levels of these parameters. A maximum DBPFP removal from 1510 to 1160 $\mu\text{g}/\text{L}$ was observed at the cell voltage of 0.6 V. For the removed DBPFP, electro-adsorption played a greater role than physical adsorption. However, it is also noted that there could be electrochemical oxidations that led to reduction of humic content and formation of new dichloroacetic acid precursors at high cell voltages. Because of the potential of CDI on reducing health risks from the formation of less brominated DBPs upon subsequent chlorination, it can be considered as a potential technology for DBP control in drinking water treatment.

© 2016 Elsevier B.V. All rights reserved.

1. Introduction

Disinfection as an essential water treatment practice for elimination of waterborne diseases brings in a variety of disinfection by-

* Corresponding author at: Department of Water Engineering and Science, College of Civil Engineering, Hunan University, Changsha, Hunan 410082, China.

E-mail address: tang@minnwater.com (H.L. Tang).

products (DBPs) in the finished water (Xie, 2004). Many DBPs have been found to have definitive adverse health impact even at low concentrations. For instance, trihalomethanes (THMs) and haloacetic acids (HAAs) are two typical classes of DBPs that have been regulated in many countries for decades. Since their formation is attributable to the reactions between the disinfectant (such as chlorine) and DBP precursors (such as natural organic matter (NOM) and bromide), processes targeting on the removal of these precursors are among the options for effective DBP control (Watson et al., 2012; Jiang et al., 2016).

Capacitive deionization (CDI) has been reported as a promising water desalination technology (Suss et al., 2015). It is based on an electro-adsorption concept that operates at a low cell voltage (0.6–1.2 V) using a pair of juxtaposed, highly porous electrodes. Due to the applied electric field, ions are removed from the water and temporarily stored in the electrical double layers (EDL) that form inside the porous electrodes. CDI is recently studied as a low-cost and easy-to-operate process for the removal of a variety of cations and anions such as heavy metals (Huang et al., 2016), bromide (Xu et al., 2008), and even the weakly charged organic matter (Wang et al., 2015). Comparing to conventional processes such as coagulation and ozonation that preferentially remove large DBP precursors with aromatic structures while having limited efficiency in eliminating small precursors (Chang et al., 2001; Chiang et al., 2002; Zhao et al., 2009), CDI appears to affect DBP precursors in a different mechanism. Xu et al. (2008) reported that the ion selectivity by CDI treatment of brackish produced water followed an order of $I > Br > Ca > \text{alkalinity} > Mg > Na > Cl$ and there was a bromide removal efficiency of 50% in their CDI study. It is well known that bromide, as an important inorganic DBP precursor in water may react with chlorine to form hypobromous acid (HOBr), which may then react with NOM and generate brominated DBPs (Zhang et al., 2008; Zhang et al., 2014) that are more toxic than their chlorinated analogues (Pals et al., 2013; Yang and Zhang, 2013; Liu and Zhang, 2014). The removal of bromide therefore may be accompanied with reductions on the formation of brominated DBPs during subsequent chlorination. Simultaneous with bromide removal, NOM – the main organic DBP precursor in water may compete with the inorganic ions for adsorption sites on the surface of the CDI electrode and impair its desalination efficiency (Gabelich et al., 2002; Mossad and Zou, 2013; Wang et al., 2015). As a result of the potential of CDI for competitively removing organic matter and bromide from water, it is critical to evaluate the effectiveness of CDI on DBP control, since the desalinated water is anticipated to be exposed to subsequent disinfection prior to human use.

In this study, humic acid (HA) as a major fraction of NOM was spiked into synthetic bromide-containing saline water to simulate inland water prior to CDI treatment. The primary objective of this study was to clarify the effects of CDI on DBP precursors during the competitive removal of HA and bromide. Water samples prior to and after CDI treatment were quantified for DBP precursors using a DBP formation potential (FP) test with chlorine, and the analyzed species of DBPFP included: four THMs (chloroform (CF), bromodichloromethane (BDCM), dibromochloromethane (DBCM), and bromoform (BF)), six HAAs (monochloroacetic acid (MCAA), monobromoacetic acid (MBAA), dichloroacetic acid (DCAA), trichloroacetic acid (TCAA), bromochloroacetic acid (BCAA), and dibromoacetic acid (DBAA)), four haloacetonitriles (HANs: dichloroacetonitrile (DCAN), trichloroacetonitrile (TCAN), bromochloroacetonitrile (BCAN), and dibromoacetonitrile (DBAN)), two haloketones (HKs: 1,1-dichloro-2-propanone (DCP) and 1,1,1-trichloro-2-propanone (TCP)), and chloral hydrate (CH). Since THMs and HAAs are the most predominant and commonly regulated DBP groups, the research into the precursors for these groups is of particular interest. This is the first study reporting the potential of CDI for DBP precursor removal.

2. Materials and methods

2.1. Chemicals

Technical grade HA was purchased from Sinopharm Chemical Reagent (Shanghai, China). Analytical grade sodium bromide (NaBr) and sodium chloride (NaCl) were purchased from Xilong Chemical Industry (Guangdong, China). Sodium hypochlorite (NaClO, reagent grade, 5%) was obtained from Sigma-Aldrich (St. Louis, MO, USA). All DBP standards were obtained from Supelco (Bellefonte, PA, USA).

2.2. Laboratory CDI experiments

A bench-scale CDI assembly was set up with one pair of pristine activated carbon cloth (ACC, FM10, Chemviron, UK) as electrodes. The ACC (0.5 g, 0.35 cm × 0.35 cm) was pre-washed with 0.01 N HCl solution and then ultra-pure water to remove any residual organics and ions. Fig. 1 shows the schematic diagram of the CDI configuration and reactor setup. The system included a CDI cell, a potentiostat as external power supply, and a magnetic stirring plate with a stirrer for sample mixing. In the CDI cell, titanium wires were attached to the ACC as current collectors. Rubber slice separators were placed between the two juxtaposed ACC to result in a channel width of 2 mm. The entire stack of all layers was bound together with a cable tie and was placed in a beaker containing 75 mL synthetic raw saline water with conductivity of 1675 $\mu\text{S}/\text{cm}$. Model water with elevated concentrations of bromide (1.78 mg/L) and HA (10 mg/L as dissolved organic carbon (DOC)) was used to simulate natural water under the influence of tributary inflows, dissolution of geological sources, and anthropogenic activities (Selcuk, 2010; Watson et al., 2012; Jiang et al., 2016). The water quality parameters of the synthetic raw water are summarized in Table 1.

Prior to each run, the cell was pre-rinsed in the raw water for 4 h to establish an equilibrium state of physical adsorption of HA and inorganic ions. A cell voltage (V_{cell}) of 0.6-, 0.9-, and 1.2 V was then applied to the CDI cell to initiate the electro-adsorption, respectively. The CDI treatment lasted 1 h prior to the sample collection. Between each run, the CDI cell was also washed with 0.01 N HCl solution and then ultra-pure water to eliminate the influence of organics and salts carryover from the previous run. To explore the effect of physical adsorption only, a control run was also performed on an open circuit ($V_{\text{cell}} = 0\text{ V}$) for 1 h.

2.3. Sample dilution and the FP test

A 5 × dilution was performed on all samples after collection. These diluted samples were then sent for DOC, UV_{254} , bromide, and DBPFP analyses. DOC was analyzed by a total organic carbon (TOC) analyzer (TOC-V CPH, Shimadzu, Japan) after passing each sample through a 0.45 μm membrane. UV_{254} was measured using a spectrophotometer (UV-1800, Shanghai Aoxi, China) equipped with a 1 cm path length

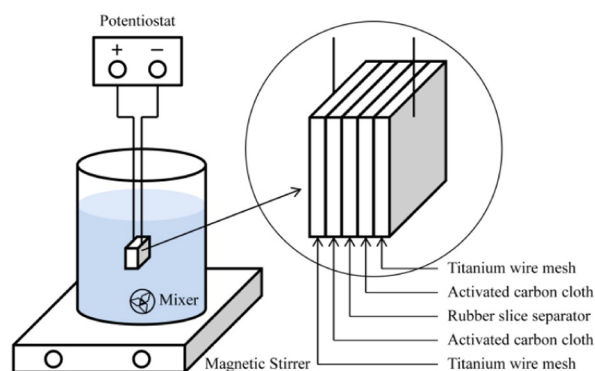


Fig. 1. Schematic diagram of CDI configuration and reactor setup.

Table 1

Water quality parameters of the raw synthetic saline water.

Parameter	pH	Conductivity [μS/cm]	DOC [mg/L]	Bromide [mg/L]	Chloride [mg/L]	SUVA ^a [L/mg-m]	Br/DOC [μg/mg]	Cl ₂ demand [mg/L]
Value	6.5	1675	9.98	1.78	607	10.9	179	19

^a SUVA: specific ultraviolet absorbance.

quartz cell. Bromide was measured with an ion chromatograph (IC) system (761, Metrohm, Switzerland) equipped with a Supp 7250/4.0 anion column using a 3.6 mM sodium bicarbonate (NaHCO₃) eluent at a flow rate of 0.8 mL/min.

To quantify organic DBP precursors, a DBPFP test was conducted by applying a chorine dose of 20 mg/L to each diluted phosphate-buffered sample at pH 7 (Singer, 1999; Tang et al., 2012). The samples (170 mL each, head-space free in amber bottles) were then incubated at 25 °C in the absence of light for 72 h. At the end of the incubation, each sample was distributed to two 40 mL glass vials pre-loaded with excess sodium thiosulfate (Na₂S₂O₃) to quench residual chlorine. The de-chlorinated samples were sealed with PTFE-lined screw caps without headspace in the glass vials. To inhibit the decomposition of DBPs (Nikolaou et al., 2000), the samples were chilled at 4 °C and extracted for DBPs within 24 h. The remaining portions of the chlorinated samples were analyzed for chlorine residuals by a Pocket Colorimeter II (Hach Company, USA) with the DPD (*N,N*-diethyl-*p*-phenylene-diamine) colorimetric method.

2.4. DBP extractions and measurements

The samples were extracted for HAA and THM/HAN/HK/CH analytes following modified EPA Methods 552.3 and 551.1, respectively. Gas chromatographs (GC, 7890A, Agilent, USA) equipped with electron capture detectors were employed for the DBP analyses. The extracted HAA analytes were separated on a DB-1701 capillary column (30 m × 0.25 mm × 0.25 μm) while the extracted THM/HAN/HK/CH analytes were separated on a DB-1 capillary column (30 m × 0.32 mm × 0.25 μm). Details on the protocols can be found elsewhere (Tang et al., 2012). The minimum reporting level (MRL) of each species was 1 μg/L. Duplicate samples were analyzed, and the data presented in this research were average of the duplicate samples.

2.5. Bromine substitution factor (BSF) calculations

The BSF was calculated as the ratio of the molar concentration of bromine incorporated in one class of DBPs to the total molar concentration of chlorine and bromine incorporated in that class (Hua and Reckhow, 2013). It is expressed as a fraction between 0 and 1. Eqs. (1) and (2) present the calculations of BSF for THMs and dihaloacetic acids (DHAAs), respectively.

$$\text{BSF(THM)} = \frac{[\text{BDCM}] + 2[\text{DBCM}] + 3[\text{BF}]}{3([\text{CF}] + [\text{BDCM}] + [\text{DBCM}] + [\text{BF}])} \quad (1)$$

$$\text{BSF(DHAA)} = \frac{[\text{BCAA}] + 2[\text{DBAA}]}{2([\text{DCAA}] + [\text{BCAA}] + [\text{DBAA}])} \quad (2)$$

3. Results and discussion

3.1. Bromide removal by CDI and its effect on BSF

The removal of bromide in the presence of HA is illustrated as the ratio of Br/DOC in Fig. 2a. The raw water had a Br/DOC ratio of 179 μg/mg. The CDI treatment was able to bring down the ratio by 26% at V_{cell} of 0.6 V, indicating the preferential removal of bromide over the weakly charged HA. A further increase of V_{cell} to 0.9 and 1.2 V led to much lower ratios till 107 μg/mg (41% reduction). This implied that higher V_{cell} in

CDI treatment promoted higher electro-adsorption of bromide, and the phenomenon was attributed to a thicker EDL and stronger Coulombic interactions between the electrodes and charged ions (Liu et al., 2015). The results also revealed that the CDI process behaved differently compared with other processes such as nanofiltration on the competitive removal of bromide and NOM. In contrast to Chellam (2000) who reported high NOM removal with poor bromide removal by

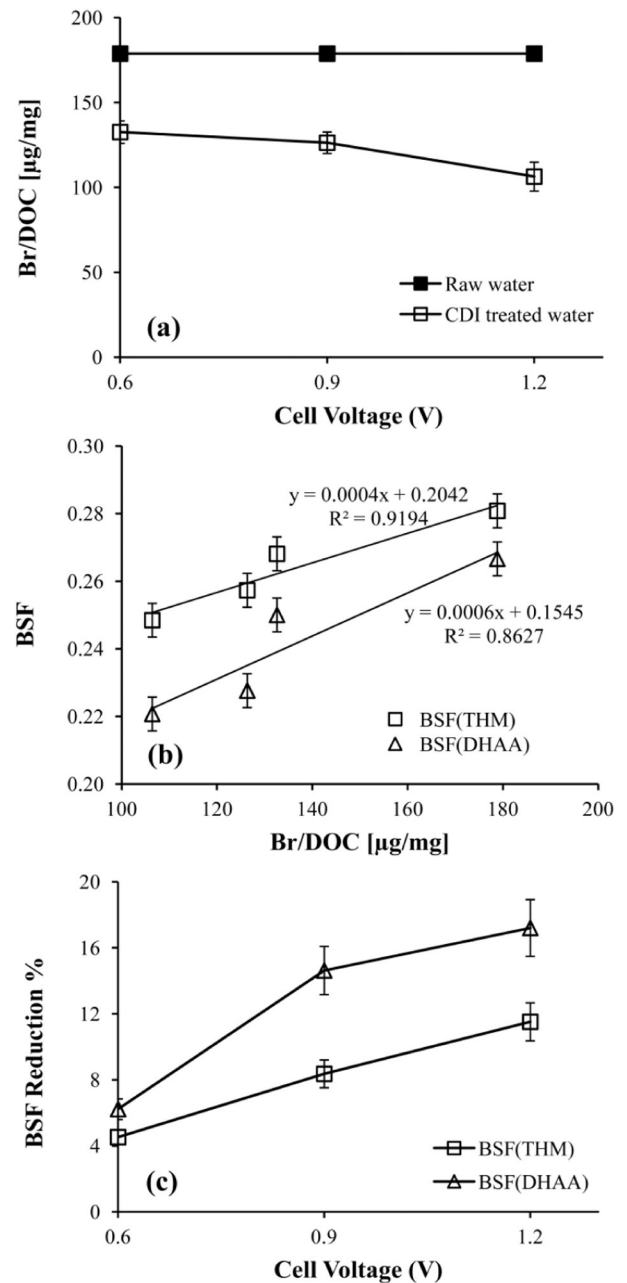


Fig. 2. Effect of CDI on Br/DOC and BSF. (a) Reduction of Br/DOC as a function of cell voltage; (b) correlations between BSF and Br/DOC; (c) BSF reduction percentages as a function of cell voltage.

nanofiltration membranes and resulted in large increases in the Br/DOC ratio, it is found in the present study that the CDI behaved oppositely. It removed more bromide and decreased the Br/DOC ratio.

The Br/DOC ratio was found linearly associated with the BSF values (Fig. 2b). The result agrees with Hu et al. (2010) who examined three Br/DOC ratios (ambient, 50, and 100 $\mu\text{g}/\text{mg}$) and found a lower ratio shifted DBP speciation toward less brominated species as indicated by BSF values. In the present study, the BSF values for THMs and DHAAs of the raw water were 0.281 and 0.267, respectively. The BSF(THM) was higher because the bromine substitution into THMs is more efficient than into DHAAs (Hua et al., 2006). Both BSF values were reduced as the CDI treatment decreased the Br/DOC ratio.

After the CDI treatment, the reduction percentage of BSF(DHAA) was greater than that of BSF(THM), and higher V_{cell} was associated with higher reduction percentages of both BSF values (Fig. 2c). The results implied easier removal of DHAA precursors than that of THM precursors during electro-adsorption. The characteristics of these precursors were discussed by Hua and Reckhow (2007) based on hydrophobicity and molecular weight (MW) of NOM. In short, THM precursors were more associated with hydrophobic, aromatic and high MW NOM fractions while DHAA precursors were more associated with hydrophilic, aliphatic and low MW NOM fractions. Since the HA molecules are negatively charged in tested pH range owing to the deprotonation of carboxyl and phenolic groups, different NOM fractions may respond differently to increased V_{cell} by CDI treatment. Therefore, it could be the easier removal of hydrophilic, aliphatic and low MW NOM fractions that explained the greater reduction percentages of BSF(DHAA) values at increased V_{cell} . Such CDI behavior was opposite to that of coagulation, which showed preferential removal of hydrophobic organic matter over hydrophilic organic matter (Kim and Yu, 2005; Hua and Reckhow, 2007; Zhao et al., 2009). It was also in contrast to that of ozonation, which increased BSF values for THMs and DHAAs (Mao et al., 2014). The BSF values for monohaloacetic acids and dihaloacetonitriles were unavailable and unrepresentative, respectively, due to either undetected or extremely low concentrations in the diluted samples. They were therefore not discussed in this study.

3.2. Organic DBP precursor removal by CDI

The level of organic DBP precursors (namely DBPFP), which was the sum of all analyzed DBPs following the FP test, was 1510 $\mu\text{g}/\text{L}$ for the raw water. The CDI treatment was able to reduce the DBPFP by 23% to 1160 $\mu\text{g}/\text{L}$ at V_{cell} of 0.6 V. However, higher V_{cell} were not associated with increased DBPFP removal. As V_{cell} increased, the DBPFP removal efficiency decreased (Fig. 3a). The phenomenon was attributed to the following reasons. Firstly, the organic DBP precursors with zero or a little charge could be competitive with inorganic ions for adsorption sites on the surface of the electrodes. As the CDI removed more inorganic ions under higher V_{cell} , the removal of organic DBP precursors was impaired. Secondly, there could be reduced interactions between cations (e.g. Na^+) and HA molecules in solution by the CDI treatment. Because these cations can be attracted to the negative carboxyl and hydroxyl groups in HA, which reduces the hydrophilic nature and provides a cation bridge that links HA to the negatively charged surface (Duan et al., 2002; Chow et al., 2005; Wang et al., 2011), the removal of these inorganic ions weakened the attraction force between the HA and the electrode, and thus led to poor removal of organic DBP precursors.

Among the analyzed DBP species following the FP tests, the following groups of DBPs were detected in this research: THMs and HAAs (the most predominant and commonly regulated DBP groups), CH, HANs and HKs. The fractions of DBP species are shown in Fig. 3b. Because TCAA and DCAA are produced as a result of different mechanistic pathways (Bond et al., 2012), their precursors are thought to be different and are therefore discussed separately in this research. The order of the DBP species fractions was THM (53%) > TCAA (17%) > DCAA (11%) > CH (4.6%) > HAN (2.0%) > HK (1.5%) in the raw water. The CDI

treatment did not change this order. However, there were noticeable changes on the fractions of some main groups of DBPs including THM, DCAA, and TCAA. At V_{cell} of 1.2 V, the THM fraction decreased from 53% to 49%, and the TCAA fraction decreased from 17% to 15%. The DCAA fraction, on the other hand, increased from 11% to 14%, which showed an opposite trend in contrast to those of THM and TCAA. Fig. 3c, which further illustrates the removal percentages of DBP species relative to their respective initial concentrations in chlorinated raw water, confirmed that the species changes were significant. The THMFP and TCAAFP removal percentages were all above zero while the DCAAFP removal percentages went from positive to negative values as V_{cell} increased. TCAA precursors are known to be similar to THM precursors in their more hydrophobic nature compared to DCAA precursors (Bond et al., 2012). In photocatalytic and photoelectrocatalytic processes (Liu et al., 2008; Li et al., 2011), greater reductions of THM and TCAA precursors than DCAA precursors were attributable to the transformation of large aromatic organics to smaller and more hydrophilic organics. In an electrochemical process only, Duan et al. (2015)

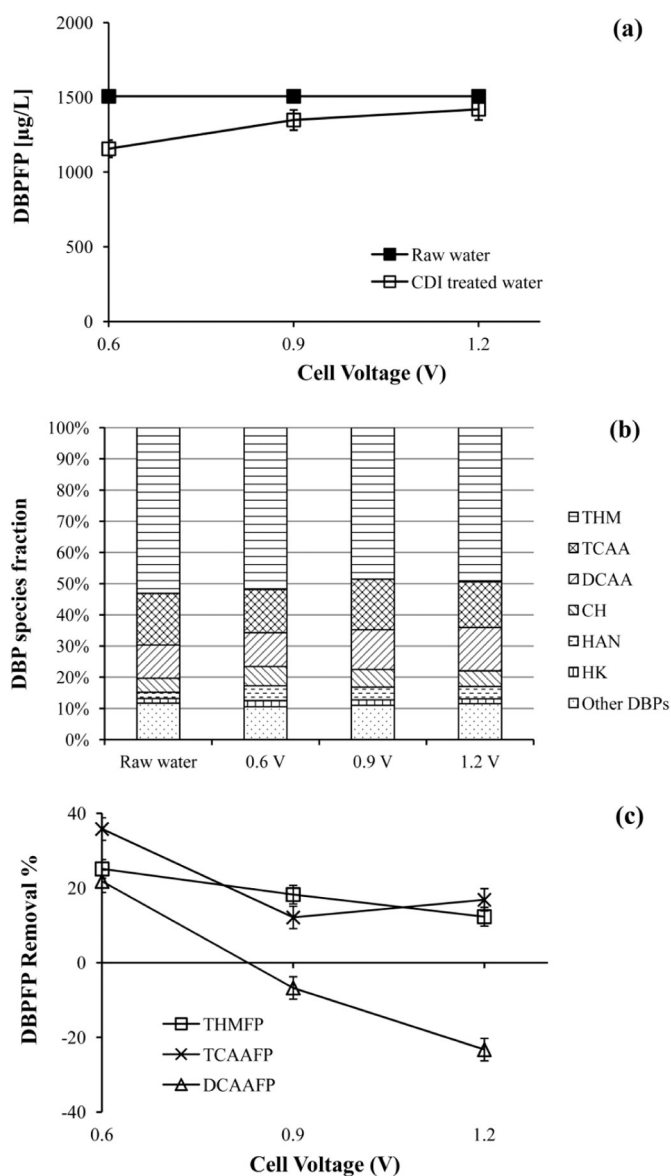


Fig. 3. Effect of CDI on DBPFP and its species fractions: (a) DBPFP as a function of cell voltage; (b) comparison of individual DBP species fractions before and after CDI treatment (other DBPs refer to the sum of MCAA, MBAA, BCAA and DBAA); (c) individual DBPFP removal percentages as a function of cell voltage.

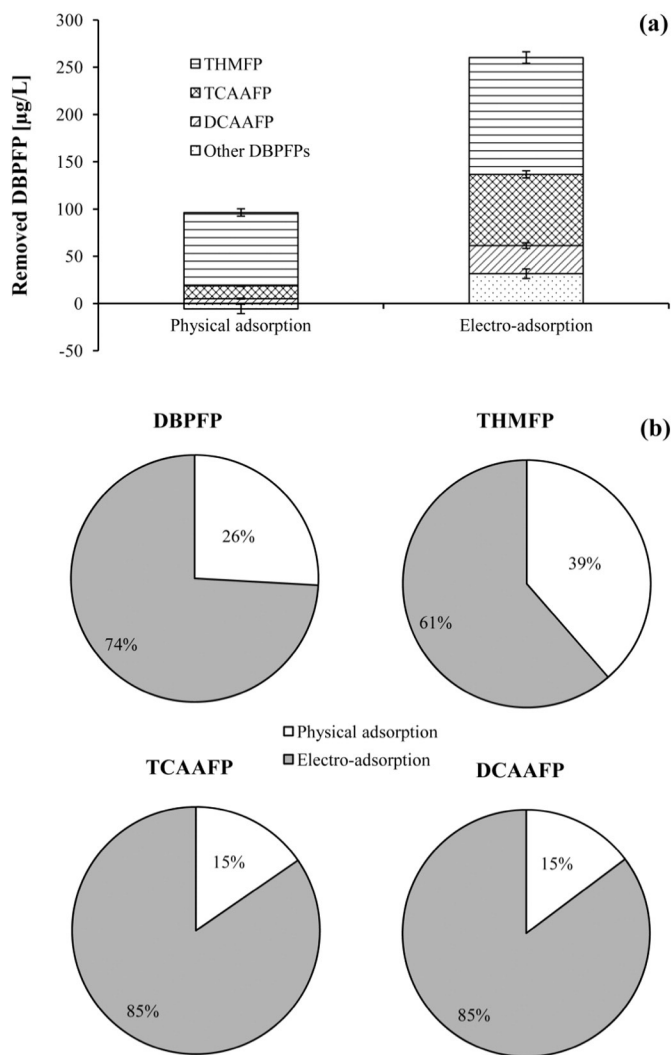


Fig. 4. Effect of physical adsorption and electro-adsorption on DBPFP at V_{cell} of 0.6 V: (a) comparison of removed fractions of DBPFP by physical adsorption and electro-adsorption; (b) percentages of physical adsorption and electro-adsorption on each DBPFP fraction.

observed a removal efficiency of 40% on phenol by electrochemical oxidations at 1.5 V. In CDI process, there was also evidence that Faradaic reactions such as oxygen reduction and Cl^- oxidation would happen at V_{cell} as low as 0.8 V (Lee et al., 2010). These reactions may induce changes in the chemistry of NOM in the solution. The electrophilic structures and unsaturated bonds in HA molecules could be attacked during partial oxidation of organic matter by these electrochemical reactions, and thus increased the carboxylic fraction that contributed to DCAA precursors in the solution.

3.3. Physical adsorption versus electro-adsorption

There are two commonly known mechanisms of ion removal during CDI process: (1) physical adsorption as a result of intrinsic affinity between the ions and the ACC surface (Ryoo and Seo, 2003); and (2) electro-adsorption as a result of the formation of EDL. Although the EDL effect is the major mechanism in CDI, physical adsorption may also play a significant role. It not only applies to inorganic ions, but also applies to the weakly charged HA. As HA is low ionized under partial acidic and neutral pH, it tends to form colloidal substance and can be adsorbed on the ACC without the influence of an external electric field, blocking the pores of CDI electrodes (Mossad and Zou, 2013). In contrast to electro-adsorption, physical adsorption is considered un-reversible

since it does not respond to desorption by shorting the electrodes or reversing the applied voltage during regeneration cycles of the CDI process (Yao and Tang, 2016), unless a chemical wash is performed for electrode regeneration.

To quantify the individual amount of physical adsorption and electro-adsorption on organic DBP precursors, a physical adsorption control experiment was performed by running the CDI process on an open circuit ($V_{\text{cell}} = 0$ V). The amount of electro-adsorption was calculated by subtracting the amount of physical adsorption at V_{cell} of 0 V from the removed DBPFP obtained from a comparative closed circuit experiment at V_{cell} of 0.6 V. A low V_{cell} of 0.6 V was used for comparison in order to prevent interferences from possible Faradaic reactions. In general, physical adsorption removed 91 $\mu\text{g/L}$ DBPFP (Fig. 4a), which contributed to 26% of the removed DBPFP (Fig. 4b). A higher percentage (74%) of the removed DBPFP was attributable to electro-adsorption. Greater portions of electro-adsorption were also observed on the target species of THMFPP (61%), TCAAFF (85%), and DCAAFF (85%) (Fig. 4b). The lower percentage of THMFPP than HAAFF in the electro-adsorbed portion might be attributable to the hydrophobic nature of THM precursors. On the other hand, among the removed DBPFP by physical adsorption, the percentage of removed THMFPP (39%) was greater than TCAAFF and DCAAFF (both at 15%). It can be deduced that physical adsorption prefers to remove the hydrophobic fraction of organics compared to electro-adsorption. Besides, a competitive adsorption mechanism may exist during the removal of different organic DBP precursors by CDI. Ayrançi and Conway (2001) explored the electro-adsorption of 2-chlorophenol and 4-chlorophenol as two model organics that were competitively present in mixture and found the presence of 4-chlorophenol would decrease the adsorption rate and extent of 2-chlorophenol. Niu and Conway (2003) also reported that the electro-adsorption of some model organics were largely reversible. The present study confirmed that the organic DBP precursors can be adsorbed by both physical and electro-adsorption mechanisms during the CDI treatment.

3.4. Adsorption versus electrochemical oxidation

Electrochemical reactions occurring at electrode surfaces of CDI at $V_{\text{cell}} \leq 1.2$ V have been reported elsewhere (Ying et al., 2002; Lee et al., 2010). In addition to the previously discussed adsorption mechanisms in Section 3.3, electrochemical oxidation of organics may also exist in CDI. In the present study, SUVA, a parameter that relates humic content with DBP formation in waters (Vermeer et al., 1998; Chen and Valentine, 2007), was employed to explore potential changes of organic DBP precursors in terms of humic content by CDI treatment. The SUVA of raw water was 10.9 L/mg-m (Fig. 5). Since there was hardly any Faradaic reaction at a low V_{cell} of 0.6 V, the reduction of SUVA to 8.0 L/mg-m

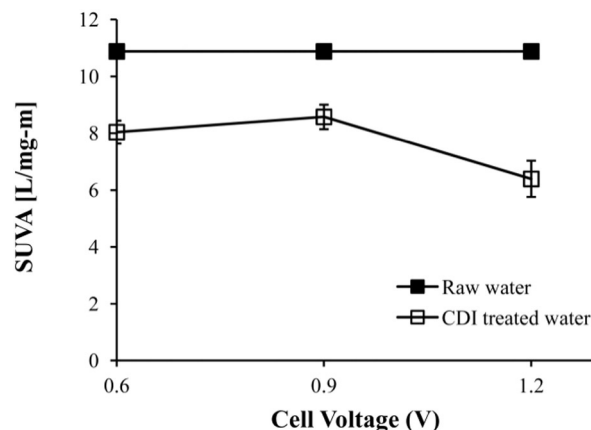


Fig. 5. Effect of CDI on SUVA.

could be mainly attributed to the adsorption mechanisms only. As was discussed in Section 3.3, electro-adsorption would remove the hydrophobic and more humic fraction of organics to a lesser extent compared to physical adsorption. Therefore, increasing the V_{cell} from 0.6 to 0.9 V would not further reduce the SUVA. However, at V_{cell} of 1.2 V, the SUVA was reduced to 6.4 L/mg-m. Interpretation to the further reduction of humic content from the raw water when V_{cell} increased from 0.9 to 1.2 V was outside the scope of the electro-adsorption mechanism. It is deduced that the further reduction of SUVA at V_{cell} of 1.2 V was related with the stronger electrochemical oxidation reactions at the electrode surfaces, which broke down the HA to less humic substances.

3.5. Implications

CDI was previously understood as a water desalination technology only. The results of the study add to the existing knowledge regarding a pool of potential technologies for DBP control in drinking water treatment. Some effects of CDI are considered beneficial. For example, being opposite from nanofiltration, CDI preferentially removes bromide over NOM. Therefore, when being used as a water pretreatment process, CDI can lead to the formation of less brominated DBPs as indicated by lower BSF and DBPFP values upon subsequent chlorination, and eventually reduce health risks exposed to drinking water users. Besides, in contrast to the conventional coagulation and ozonation processes that remove low MW, aliphatic, and hydrophilic fraction of organics to a lesser extent, CDI is responsive to the removal of such fraction as a result of an electro-adsorption mechanism. On the other hand, adverse effects of CDI are also implied in this study. Firstly, operation of CDI may lead to an explicit electrochemical oxidation effect similar to that of photocatalytic and photoelectrocatalytic processes that changes the NOM structure and increases the carboxylic fraction in solution that contributes to new DCAA precursors. These electrochemical reactions are also known to expedite electrode aging (Gao et al., 2015). Secondly, physical adsorption of NOM is known to cause fouling on the electrodes (Mossad and Zou, 2013). These adverse effects would make CDI unsustainable and inefficient. It is also noted that the extent of DBP precursor removal by CDI process alone is limited. For better performance, CDI could be used in combination with other processes for more efficient DBP control in drinking water treatment. Research remains to be done regarding the potential influences from different inorganic and organic constituents in raw water, since CDI selectivity for different ions (Mossad and Zou, 2012), alkalinity (Xu et al., 2008), and hardness (Seo et al., 2010) were reported. Besides, while the present study started with pristine ACC electrodes, it has been discovered that the corrosion of positive electrodes may negatively impact the CDI process (Cohen et al., 2013). Since the negatively charged HA molecules owing to the deprotonation of carboxyl and phenolic groups are retained by the positive electrodes, the deterioration of positive electrodes after repeated uses may consistently impact the performance of DBP precursor removal. Future studies will include the scope of these areas to obtain a thorough picture on their respective influence on DBP precursors.

4. Conclusions

CDI is a complex process and the investigation into its DBP precursor removal potential is important for subsequent disinfection in drinking water treatment. It was found in this study that CDI could reduce both inorganic and organic DBP precursors as revealed by the preferential removal of bromide over NOM, the reduction of BSF values, and the lowered DBPFP. For the removed DBPFP, electro-adsorption was found to play a greater role than physical adsorption. Besides the two commonly known adsorption mechanisms in CDI, there were potential electrochemical oxidations that led to the reduction of humic content and formation of new DCAA precursors. Because of the potential of CDI on reducing health risks from the formation of less brominated DBPs

upon subsequent chlorination, it can be considered as a potential technology for DBP control in drinking water treatment.

Acknowledgements

This research was supported by Minn Water (Minneapolis, MN, USA) under project no. 1390501914. Danyang Liu acknowledged the research staff at School of Environment at Tsinghua University for providing training to access research facilities.

References

- Ayranci, E., Conway, B.E., 2001. Removal of phenol, phenoxide and chlorophenols from waste-waters by adsorption and electrosorption at high-area carbon felt electrodes. *J. Electroanal. Chem.* 513, 100–110.
- Bond, T., Goslan, E.H., Parsons, S.A., Jefferson, B., 2012. A critical review of trihalomethane and haloacetic acid formation from natural organic matter surrogates. *Environ. Technol. Rev.* 1, 93–113.
- Chang, E.E., Chiang, P.C., Ko, Y.W., Lan, W.H., 2001. Characteristics of organic precursors and their relationship with disinfection by-products. *Chemosphere* 44, 1231–1236.
- Chellam, S., 2000. Effects of nanofiltration on trihalomethane and haloacetic acid precursor removal and speciation in waters containing low concentrations of bromide ion. *Environ. Sci. Technol.* 34, 1813–1820.
- Chen, Z., Valentine, R.L., 2007. Formation of N-nitrosodimethylamine (NDMA) from humic substances in natural water. *Environ. Sci. Technol.* 41, 6059–6065.
- Chiang, P.C., Chang, E.E., Liang, C.H., 2002. NOM characteristics and treatabilities of ozonation processes. *Chemosphere* 46, 929–936.
- Chow, A.T., Guo, F., Gao, S., Breuer, R., Dahlgren, R.A., 2005. Filter pore size selection for characterizing dissolved organic carbon and trihalomethane precursors from soils. *Water Res.* 39, 1255–1264.
- Cohen, I., Avraham, E., Bouhadana, Y., Soffer, A., Aurbach, D., 2013. Long term stability of capacitive de-ionization processes for water desalination: the challenge of positive electrodes corrosion. *Electrochim. Acta* 106, 91–100.
- Duan, J., Wilson, F., Graham, N., Tay, J.H., 2002. Adsorption of humic acid by powdered activated carbon in saline water conditions. *Desalination* 151, 53–66.
- Duan, F., Li, Y., Cao, H., Wang, Y., Crittenden, J.C., Zhang, Y., 2015. Activated carbon electrodes: electrochemical oxidation coupled with desalination for wastewater treatment. *Chemosphere* 125, 205–211.
- Gabelich, C.J., Tran, T.D., Suffet, I.H., 2002. Electrosorption of inorganic salts from aqueous solution using carbon aerogels. *Environ. Sci. Technol.* 36, 3010–3019.
- Gao, X., Omosebi, A., Landon, J., Liu, K., 2015. Surface charge enhanced carbon electrodes for stable and efficient capacitive deionization using inverted adsorption-desorption behavior. *Energy Environ. Sci.* 8, 897–909.
- Hu, J., Song, H., Karanfil, T., 2010. Comparative analysis of halonitromethane and trihalomethane formation and speciation in drinking water: the effects of disinfectants, pH, bromide, and nitrite. *Environ. Sci. Technol.* 44, 794–799.
- Hua, G., Reckhow, D.A., 2007. Characterization of disinfection byproduct precursors based on hydrophobicity and molecular size. *Environ. Sci. Technol.* 41, 3309–3315.
- Hua, G., Reckhow, D.A., 2013. Effect of pre-ozonation on the formation and speciation and DBPs. *Water Res.* 47, 4322–4330.
- Hua, G., Reckhow, D.A., Kim, J., 2006. Effect of bromide and iodide ions on the formation and speciation of disinfection byproducts during chlorination. *Environ. Sci. Technol.* 40, 3050–3056.
- Huang, Z., Lu, L., Cai, Z., Ren, Z.J., 2016. Individual and competitive removal of heavy metals using capacitive deionization. *J. Hazard. Mater.* 302, 323–331.
- Jiang, Y., Goodwill, J.E., Tobiasson, J.E., Reckhow, D.A., 2016. Bromide oxidation by ferrate(VI): the formation of active bromine and bromate. *Water Res.* 96, 188–197.
- Kim, H.-C., Yu, M.-J., 2005. Characterization of natural organic matter in conventional water treatment processes for selection of treatment processes focused on DBPs control. *Water Res.* 39, 4779–4789.
- Lee, J.-H., Bae, W.-S., Choi, J.-H., 2010. Electrode reactions and adsorption/desorption performance related to the applied potential in a capacitive deionization process. *Desalination* 258, 159–163.
- Li, A., Zhao, X., Liu, H., Qu, J., 2011. Characteristic transformation of humic acid during photoelectrocatalysis process and its subsequent disinfection byproduct formation potential. *Water Res.* 45, 6131–6140.
- Liu, J., Zhang, X., 2014. Comparative toxicity of new halophenolic DBPs in chlorinated saline wastewater effluents against a marine alga: halophenolic DBPs are generally more toxic than haloaliphatic ones. *Water Res.* 65, 64–72.
- Liu, S., Lim, M., Fabris, R., Chow, C., Drikas, M., Amal, R., 2008. TiO_2 photocatalysis of natural organic matter in surface water: impact on trihalomethane and haloacetic acid formation potential. *Environ. Sci. Technol.* 42, 6218–6223.
- Liu, D., Huang, K., Xie, L., Tang, H.L., 2015. Relation between operating parameters and desalination performance of capacitive deionization with activated carbon electrodes. *Environ. Sci. Technol.* 1, 516–522.
- Mao, Y., Wang, X., Yang, H., Wang, H., Xie, Y.F., 2014. Effects of ozonation on disinfection byproduct formation and speciation during subsequent chlorination. *Chemosphere* 117, 515–520.
- Mossad, M., Zou, L., 2012. A study of the capacitive deionisation performance under various operational conditions. *J. Hazard. Mater.* 213–214, 491–497.
- Mossad, M., Zou, L., 2013. Study of fouling and scaling in capacitive deionisation by using dissolved organic and inorganic salts. *J. Hazard. Mater.* 244, 387–393.

- Nikolaou, A.D., Golfinopoulos, S.K., Kostopoulou, M.N., 2000. Decomposition of dihaloacetonitriles in water solutions and fortified drinking water samples. *Chemosphere* 41, 1149–1154.
- Niu, J., Conway, B.E., 2003. Adsorption of organics onto a high-area C-cloth electrode from organic solvents and organic solvent/water mixtures. *J. Electroanal. Chem.* 546, 59–72.
- Pals, J., Attene-Ramos, M., Xia, M., Wagner, E.D., Plewa, M.J., 2013. Human cell toxicogenomic analysis linking reactive oxygen species to the toxicity of monohaloacetic acid drinking water disinfection byproducts. *Environ. Sci. Technol.* 47, 12514–12523.
- Ryoo, M.-W., Seo, G., 2003. Improvement in capacitive deionization function of activated carbon cloth by titania modification. *Water Res.* 37, 1527–1534.
- Selcuk, H., 2010. Disinfection and formation of disinfection by-products in a photoelectrocatalytic system. *Water Res.* 44, 3966–3972.
- Seo, S.-J., Jeon, H., Lee, J.K., Kim, G.-Y., Park, D., Nojima, H., Lee, J., Moon, S.-H., 2010. Investigation on removal of hardness ions by capacitive deionization (CDI) for water softening applications. *Water Res.* 44, 2267–2275.
- Singer, P.C., 1999. Humic substances as precursors for potentially harmful disinfection by-products. *Water Sci. Technol.* 40, 25–30.
- Suss, M., Porada, S., Sun, X., Biesheuvel, M., Yoon, J., Presser, V., 2015. Water desalination via capacitive deionization: what is it and what can we expect from it? *Energy Environ. Sci.* 8, 2296–2319.
- Tang, H.L., Chen, Y.-C., Regan, J.M., Xie, Y.F., 2012. Disinfection by-product formation potentials in wastewater effluents and their reductions in a wastewater treatment plant. *J. Environ. Monit.* 14, 1515–1522.
- Vermeer, A.W.P., van Riemsdijk, W.H., Koopal, L.K., 1998. Adsorption of humic acid to mineral particles: 1. Specific and electrostatic interactions. *Langmuir* 14, 2810–2819.
- Wang, J.H., Han, X.J., Ma, H.R., Ji, Y.F., Bi, L.J., 2011. Adsorptive removal of humic acid from aqueous solution on polyaniline/attapulgite composite. *Chem. Eng. J.* 173, 171–177.
- Wang, C., Song, H., Zhang, Q., Wang, B., Li, A., 2015. Parameter optimization based on capacitive deionization for highly efficient desalination of domestic wastewater biotreated effluent and the fouled electrode regeneration. *Desalination* 365, 407–415.
- Watson, K., Farre, M.J., Knight, N., 2012. Strategies for the removal of halides from drinking water sources, and their applicability in disinfection by-product minimization: a critical review. *J. Environ. Manag.* 110, 276–298.
- Xie, Y.F., 2004. *Disinfection Byproducts in Drinking Water: Formation, Analysis, and Control*. FL, Lewis Publishers, Boca Raton.
- Xu, P., Drewes, J.E., Heil, D., Wang, G., 2008. Treatment of brackish produced water using carbon aerogel-based capacitive deionization technology. *Water Res.* 42, 2605–2617.
- Yang, M., Zhang, X., 2013. Comparative developmental toxicity of new aromatic halogenated DBPs in a chlorinated saline sewage effluent to the marine polychaete *Platynereis dumerilii*. *Environ. Sci. Technol.* 47, 10868–10876.
- Yao, Q., Tang, H.L., 2016. Occurrence of re-adsorption in desorption cycles of capacitive deionization. *J. Ind. Eng. Chem.* 34, 180–185.
- Ying, T.Y., Yang, K.L., Yiacoumi, S., Tsouris, C., 2002. Electrosorption of ions from aqueous solutions by nanostructured carbon aerogel. *J. Colloid Interface Sci.* 250, 18–27.
- Zhang, X.R., Talley, J.W., Boggess, B., Ding, G.Y., Birdsell, D., 2008. Fast selective detection of polar brominated disinfection byproducts in drinking water using precursor ion scans. *Environ. Sci. Technol.* 42, 6598–6603.
- Zhang, H., Zhang, Y., Shi, Q., Zheng, H., Yang, M., 2014. Characterization of unknown brominated disinfection byproducts during chlorination using ultrahigh resolution mass spectrometry. *Environ. Sci. Technol.* 48, 4396–4402.
- Zhao, H., Liu, H.J., Hu, C.Z., Qu, J.H., 2009. Effect of aluminum speciation and structure characterization on preferential removal of disinfection byproduct precursors by aluminum hydroxide coagulation. *Environ. Sci. Technol.* 43, 5067–5072.